

OPERATIONS

CYCLOTRON OPERATING SUMMARY

D.R. Poe, H.A. Thulin and P.S. Miller

K500 Operation

The K500 was operated in March and August to perform experiments which could not be scheduled in 1988. During the rest of 1989, efforts were focussed on the operation of the K1200. Table I gives the operating time statistics. These data reflect the difficulty of bringing the K500 back into operation after a long shutdown.

Table II shows the various beams which were run on the K500.

K1200 Operation

During 1989, the K1200 began to run experiments in a somewhat routine manner, and the responsibility for operating and maintaining the K1200 shifted to the Operations group. Nine K1200 experiments were run in 1989. (See Table V).

Tables III and IV show data pertinent to the K1200. Start up for new beams is straightforward, typically taking 6 to 12 hours depending on whether the beam has been run previously. This had made it possible to perform excitation functions.

We accelerated diatomic molecules (H-He) 1+ and (D-He) 1+ so as to provide lower energy beams for detector calibration than could be accelerated as atomic ions (see Table IV).

K1200 shutdowns occurred in January, March, June and August so that improvements and repairs could be made to the resonators, transmitters and the liquid helium system.

The RF system has been improving in reliability through the year (see the relevant RF articles for details). The C transmitter was redesigned to use a Thomson TH555 as a final amplifier tube, with plans to convert the other two amplifiers this year. The new transmitter

TABLE I K500 Time Distribution

	Hours	
Operation		
Research	560.5	36.6%
Development	8.0	0.5
Overhead	302.0	19.7
Maintenance	8.0	0.5
Breakdown	652.0	42.7
TOTAL	1530.5	100.0
OFF	7229.5	

TABLE II K500 BEAMS 1989

Ion	E/A [MeV/u]	Hours	% Time
$^3\text{He}^{1+}$	35.0	5.0	0.9
$^4\text{He}^{1+}$	25.0	5.8	1.0
$^{12}\text{C}^{3+}$	25.0	24.3	4.1
$^{12}\text{C}^{5+}$	40.0	11.5	2.0
$^{14}\text{N}^{6+}$	50.0	131.5	22.5
$^{14}\text{N}^{6+}$	35.0	56.7	9.7
$^{20}\text{Ne}^{4+}$	15.0	2.8	0.5
$^{36}\text{Ar}^{11+}$	35.0	159.5	27.3
$^{36}\text{Ar}^{12+}$	35.0	2.5	0.4
$^{36}\text{Ar}^{5+}$	8.0	180.3	30.8
$^{86}\text{Kr}^{8+}$	2.5	15.8	2.7
		584.8	100.0

design for the K1200 was developed using the existing transmitter as the prototype. This work has progressed as far as completing the design, testing, and ordering the parts. The modifications will be completed by mid 1990.

TABLE III K1200 Time Distribution

Operation	Hours	
Research	1312.5	28.0%
Development	284.25	6.1
Overhead	948.75	20.3
	<u>2545.5</u>	<u>54.4</u>
Maintenance	142.5	3.0
Breakdown	1998.0	42.6
TOTAL	<u>4684.0</u>	<u>100.0</u>
OFF	4075.0	

The injection of beam from the ECR source has been greatly improved by studying the beam optics and adding appropriate steering elements and magnetic shielding. It is now possible to inject ions which require the full bending power of the magnet for their acceleration. Subsequently, 40 and 50 MeV/u Kr and Xe beams were developed. (See Table IV.)

Overall K1200 reliability improved greatly as the year progressed and was over 80% during the final quarter.

TABLE IV K1200 BEAMS 1989

Ion	E/A [MeV/u]	Hours	% Time
$^4\text{He}^{1+}$	40.0	29.3	2.1
$(\text{D-He})^{1+}$	20.0	6.0	0.4
$(\text{H-He})^{1+}$	30.0	14.5	1.0
$^{14}\text{N}^{4+}$	60.0	55.0	4.0
$^{14}\text{N}^{5+}$	75.0	16.0	1.2
$^{14}\text{N}^{5+}$	80.0	50.3	3.6
$^{14}\text{N}^{6+}$	100.0	13.5	1.0
$^{20}\text{Ne}^{6+}$	65.0	19.3	1.4
$^{20}\text{Ne}^{7+}$	85.0	136.0	9.8
$^{28}\text{Si}^{5+}$	31.0	15.8	1.1
$^{40}\text{Ar}^{7+}$	30.0	85.0	6.1
$^{40}\text{Ar}^{10+}$	45.0	122.8	8.9
$^{40}\text{Ar}^{11+}$	55.0	94.0	6.8
$^{40}\text{Ar}^{12+}$	65.0	387.1	28.0
$^{40}\text{Ar}^{13+}$	75.0	15.3	1.1
$^{40}\text{Ar}^{14+}$	85.0	24.3	1.8
$^{56}\text{Fe}^{13+}$	50.0	3.0	0.2
$^{86}\text{Kr}^{20+}$	50.0	8.8	0.6
$^{129}\text{Xe}^{20+}$	22.7	41.3	3.0
$^{129}\text{Xe}^{23+}$	31.0	196.5	14.2
$^{129}\text{Xe}^{26+}$	40.0	45.5	3.3
$^{129}\text{Xe}^{30+}$	50.0	3.5	0.3
		<u>1382.3</u>	<u>100.0</u>

TABLE V K1200 Experiments 1989

MONTH	EXPT. NO.	SPOKESPERSON	BEAMS	
			ion	MeV/u
Jan.	88004	Loveland	^{129}Xe	23
Jan.-Feb.	86040	Gong	^{129}Xe	31
			^4He	40
Feb.	88012	Ogilvie	^{40}Ar	45
Apr.-May	"	"	"	55
			"	65
			"	75
			"	85
May	88003	Becchetti	^{20}Ne	85
June-July	88035	Viola	^{14}N	60
			"	80
			"	100
Sept.	88028	Morrissey	^{14}N	75
Sep.-Oct.	88014	Clayton	^{14}N	75
			^{20}Ne	65
			^{40}Ar	65
			^{40}Ar	65
Nov.	88017	Chen	^{40}Ar	65
Dec.	88027	Sarantites	^{40}Ar	65
			"	45
			"	30
			^{129}Xe	31
			^{129}Xe	40

OPERATION TROUBLE REPORT SYSTEM

P.S. Miller and R. Morin

As one means of improving the operating reliability of our cyclotrons we have organized a system for reporting, investigating and correcting technical problems that interfere with operation of the cyclotron facility. The system responds to a trouble by seeking its cause (which may not be apparent without some analysis), designing and implementing a correction, and verifying that the correction performed works. A record of the investigation and conclusions is saved in a computer data base and on paper. Information can be retrieved and processed in various ways to help answer questions from the data in trouble reports and to aid in searching for related information in log books.

Every trouble reported will be investigated. Anyone may insert a trouble report into the system by writing a brief description of the trouble. One staff member is assigned to be the investigator for the trouble report. The investigator is responsible for correction of the cause of the trouble. The investigator's objectives are:

- 1) Determine what caused the trouble, looking for things that may cause a repetition in the future;
- 2) Plan a course of action to correct the problem;
- 3) Discuss the plan with a reviewer.
- 4) Carry out the plan and verify that it works.

The reviewer is appointed at the same time as the investigator and is responsible for pointing out any difficulties that the planned corrective actions might create in some related system. When the reviewer and the investigator agree on the action plan the investigator proceeds with its implementation.

The committee that assigns the investigator and reviewer may leave a trouble report "unassigned" if the circumstances do not warrant assigning an investigator. The report is recorded for future reference and left open.

The investigator writes a report which is read by a review committee and is saved. The report is intended to be self-contained and to state conclusions such as location of the failure, cause of the failure, result of corrective action taken, etc. The summary page for a completed trouble report is shown in Fig. 1. It contains the information entered into the computer data base. Additional sheets, if any, in the report are attached to it and saved on paper.

The work performed by investigators and reviewers is administered by departments as part of the regular work load. The trouble report goes via the department to the investigator or the reviewer. Department managers control the priority of this work in relation to other assignments the employee has received.

Maintenance of trouble report data in a computer data base permits easy review when seeking to discover patterns or trends and assists in keeping up to date records of investigation status. When a trouble report is initiated it is assigned to one of eight major facilities. This coarse categorization is further refined after the report is investigated and the specific problem identified. For example, a trouble after investigation could be assigned to K1200/Vacuum System/Turbo Pumps. If at a later date we were interested in all troubles that have involved Vacuum Systems they could be quickly located regardless of the major facility they serve. The distribution of the 139 reports recorded so far is: K1200 - 45%, K500 - 6%, ECR/Injection - 8%, Beamline - 1%,

Experimental Equipment - 1%, Control System - 16%, Utilities - 14% and Other - 9%.

After a trouble is investigated it is also assigned to one of eight cause categories. This permits rapidly locating all troubles attributed to one of these major trouble contributors. If a pattern is discovered we can increase our emphasis in the area to reduce this type of failure. The distribution of the 70 reports that have been assigned a cause so far is: Assembly - 13%, Construction - 3%, Design - 19%, Information - 14%, Maintenance - 10%, Other - 10%, Unknown - 7%, and Wear Out - 9%. The 19% attributed to Design is expected to be markedly lower in future years, since the majority of the equipment monitored is being operated for the first time. Next year we would expect to see a lower proportion of design-associated problems.

Use of the computer data base also permits location of all reports that have user-specified

key words used in the description of the trouble or in a field designated to hold key words. For example, it might be of interest to locate all troubles that used the word "fuse" or the acronym "LCW" in describing the trouble. For the 139 troubles currently reported the word "fuse" appears in the trouble description in 5 of them and "LCW" in 7. After locating reports by using key words the subset can be further restricted or the included reports reviewed in detail to gain the insight desired.

Trouble reports move through six phases: Initiate, Analyze, Correct, Verify, Complete, and Close. The use of phases helps to be sure action is being taken to locate and correct the causes of our troubles. The current distribution is: Initiate - 29%, Analyze - 14%, Correct - 6%, Verify - 3%, Complete - 5%, and Closed - 44%.

BECAUSE
THEY
WERE ONES
SON -

WE
SANDING
K-2
SON
WEING
ATTORNEY
HE ON

#10

#10

TRouble REPORT - K1200 "B" LOWER SHORT SPARKS

Al
For sev
the spa
and on
inspec
improp
prompt
and the
disass
Two ca
they ha
heating

Cl
While
lower
found
a flat
"B" low
stem c
also ti
are ref
be insp

V
Since
finger

**NSCL Operations
Trouble Report**

Serial Number: 10

Date trouble observed: 9/20/89 **Time trouble observed:** 09:00
Observed by: Brandon
Trouble report written by: Poe **Date:** 9/21/89
Facility: K1200
Description of trouble:

There had been lower short sparks indicated while running. Inspection showed burning on B lower short where inner finger bar attaches to short. Short was removed and repaired. Loose connecting bolts?

Subject: K1200 B lower short sparks
Keywords: Loose screw, sliding short, spark detector
Investigator: Otterson **Reviewer:** Vincent **Assigned:** 10/9/89

Summary of analysis: **Date:** 10/17/89

Damage to B lower sliding short inner conductor finger ring was due to loose bolts apparently from improper assembly. Also due to disconnected spark detectors.

Trouble Category: 1.1.7 **Cause:** Assembly

Summary of correction: **Date:** 10/17/89

Surfaces were cleaned up and repaired. New screws with flat and lock washers were installed on all lower stems.

Summary of verification: **Date:** 10/17/89

No sparks have been seen since fix.

Date Closed: 11/30/89

Fig. 1 Completed trouble report.

K1200 MAGNET STATUS: INDUCTANCE MEASUREMENT, TEMPERATURE EFFECTS AND MODIFICATIONS

G. Humenik, J. Kuchar, A. McCartney and P. Miller

Inductances of the K1200 Cyclotron Magnet

The K1200 superconducting cyclotron magnet coils are divided in two parts. Strong inductive coupling between the two electric circuits complicates the operation of the current regulating power supply, and gives rise to a charging mode, called "current swapping", which can rapidly change the currents in the two sections of the coil in opposite directions. We wanted to find out how fast this process can occur and determine how fast the control program that checks to see that the currents are within the allowed operating region has to respond.

Analysis of Two Coupled Coils

The equivalent circuit for the magnet, its power supply and other external components, such as leads and dump resistors, is found in Fig. 1.

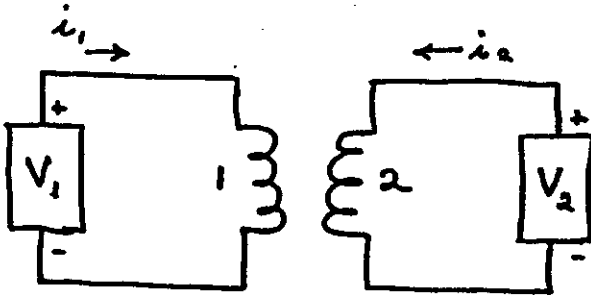


Fig. 1 Cyclotron magnet equivalent circuit.

The self inductances (L_1 and L_2) and mutual inductance (M) relate the coil voltages to the currents by the following coupled equations:

$$L_1 \frac{dI_1}{dt} + M \frac{dI_2}{dt} = V_1 \quad (1)$$

$$M \frac{dI_1}{dt} + L_2 \frac{dI_2}{dt} = V_2 \quad (2)$$

We assume that the inductances can be approximated as constants. We know that the inductance varies in both of the cyclotrons due to progressive saturation of the iron poles and yoke as the currents in the coils are increased, especially at low magnetic field. This approximation limits the validity of numerical results for any given set of inductances to current values not too far from the values for which the inductances were determined. The formal solution for the rate of change of current, provided $L_1 L_2$ is not equal to M^2 , is

$$\frac{dI_1}{dt} = (L_2 V_1 - M V_2) / (L_1 L_2 - M^2), \text{ and } (3)$$

$$\frac{dI_2}{dt} = (L_1 V_2 - M V_1) / (L_1 L_2 - M^2). \quad (4)$$

If the inductances are known the maximum dI/dt for each coil can be calculated directly by substituting the power supply clipping voltages into Eqs. (3) and (4), provided that $L_1 L_2$ does not equal M^2 .

The mutual inductance is sometimes expressed in terms of a coupling coefficient k , defined as follows:

$$M = k (L_1 L_2)^{1/2}, \quad (5)$$

where k can be shown to lie between 0 and 1. Physically, $k=1$ represents fully coupled coils, where all magnetic flux produced by current in one coil links through the other. We see that the denominator in equations (3) and (4) is zero if $k=1$. This implies that a finite applied voltage would result in an infinite dI/dt . Since k is significantly less than unity in the cyclotron magnets the rate of change of current in the magnet is finite for any finite coil voltages.

The dimensionless ratio

$$k = L_2 / L_1 \quad (6)$$

and the equivalent total inductance of both coils in series,

$$L_{tot} = L_1 + 2M + L_2, \quad (7)$$

are also of interest.

Application to the K1200 Magnet

We want to use Eqs. (1) and (2) to determine the inductances of the K1200 magnet experimentally. The data in Table I were recorded by hand while the currents were ramped by the power supply to the target currents given in the table. The charging cycle followed during this experiment is depicted in Fig. 2 as a triangle starting and ending at $I_\alpha, I_\beta = 700, 700$ A. The currents are in the normal operating region of the cyclotron. The maximum excitation allowed is $I_\alpha, I_\beta = 833.4, 884.4$ A.

Eqs. (8)-(13) below come from substituting the data from Table I into Eqs. (1) and (2).

Table I-- K1200 data near 700 A

I_α [A]	I_β [A]	V_α [V]	V_β [V]	dI_α/dt [A/s]	dI_β/dt [A/s]
700	700	25	-38	1.6	-3.25
740	580	-38.0	-8.18	-0.738	0.436
640	640	37.2	20.2	0.407	0.391
700	700				

I beta [A]

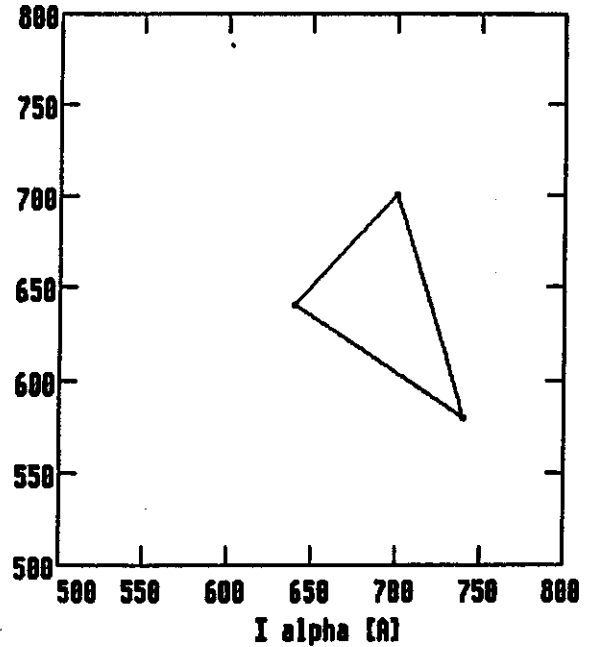


Fig. 2 Charging cycle, 700 A data

$$L_\alpha (1.6) + M (-3.25) + L_\beta (0) = 25 \quad (8)$$

$$L_\alpha (0) + M (1.6) + L_\beta (-3.25) = -38 \quad (9)$$

$$L_\alpha (-0.738) + M (0.436) + L_\beta (0) = -38 \quad (10)$$

$$L_\alpha (0) + M (-0.738) + L_\beta (0.436) = -8.18 \quad (11)$$

$$L_\alpha (0.407) + M (0.391) + L_\beta (0) = 37.2 \quad (12)$$

$$L_\alpha (0) + M (0.407) + L_\beta (0.391) = 20.2 \quad (13)$$

Any three of these equations may be solved for the inductances. The results of solving 4 sets of 3 simultaneous equations are given in Table II.

The consistency of the results obtained from solving equations from different parts of the charging cycle suggests that this method of calculating inductances is valid and could be used to investigate how the inductances vary with excitation.

Table II -- K1200 inductances, 700 A

Eqs. solved	L_{α}	M	L_{β}	k	λ
(8),(9),(10)	66.3	24.9	24.0	0.624	0.362
(11),(12),(13)	66.6	25.8	24.9	0.634	0.374
(9),(10),(12)	66.7	25.7	24.3	0.638	0.364
(8),(11),(13)	68.0	25.8	24.9	0.627	0.379

The maximum rate of change of current can be calculated from the inductances and Eq. (3) and (4), assuming that the power supply voltages are limited to + and - 40 volts on both coils. Using the inductances from the first line in Table II the results are

$$\text{Max. } dI_{\alpha}/dt = 2.0 \text{ [A/s]}, \quad (14)$$

and

$$\text{Max. } dI_{\beta}/dt = 3.8 \text{ [A/s]}. \quad (15)$$

The control program cycle time is 2 s. At present, 3 successive readings of the currents outside the magnet operating limits will cause a shut down. The delay time for this is between 4 and 6 s.

Analysis of the low current measurements given below shows that dI/dt values during current swapping at low current are smaller than those given by Eqs. (14) and (15).

Measurement of Inductances over a Range of Currents.

We later measured inductances at lower currents, where the inductances change rapidly. Such information on the variation of inductances may help improve the power supply performance (project planned for 1990). At present the stability of the current regulating system is

not satisfactory in the "+- current mode" needed for high energy cyclotron beams.

The general method described above for the 700 A inductance measurement was applied over a range of currents from 8A to 400 A. Certain details were changed for convenience and efficiency of making a large number of measurements manually. The charging cycle was always started from equilibrium at the operating point where the inductance values were desired. From each point two charging cycles were performed with constant coil voltages, 12.0 and 6.00 volts for V_{α} and V_{β} , respectively, on the first cycle and 5.00 and 10.0 volts on the second. The same voltages were used on every measurement. The voltages were held constant by the power supply; when the dI/dt values were observed to reach a constant value (within .001 A/s) the values were recorded. Then the charging cycle was stopped manually and the power supply currents were set to the initial values for the next measurement.

At each operating point the above procedure provided data for 4 groups of three equations which were solved for the inductances. The average of the 4 values of L_{α} is taken as the best estimate of the inductance at the operating point, and similarly for L_{β} and M. Data and inductance values are found in Table III.

The graph in Fig. 3 shows the results, where the inductances plotted are only those measurements with $I_{\alpha} = I_{\beta}$. In Fig. 4 some ratios of inductances from the same group of data are shown. The data plotted in Fig. 3-4 are marked with an asterisk in Table III. In Table III, dia1 and dib1 are measured dI/dt values for alpha and beta, respectively, when $V_{\alpha}=12.0$ volts and $V_{\beta}=6.0$ volts. Dia2 and dib2 represent dI/dt when $V_{\alpha}=5.0$ and $V_{\beta}=10.0$ volts.

Measurements were made at several different values of I_{α} and I_{β} which have the same "effective current" I_{eff} given by

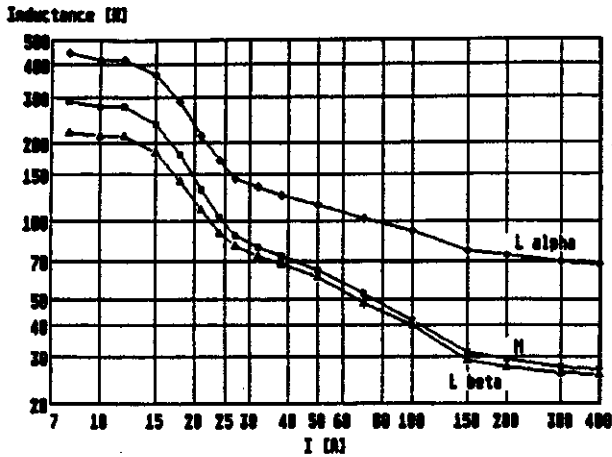


Fig. 3 Average inductance from Table III vs. current ($I_\alpha = I_\beta$).

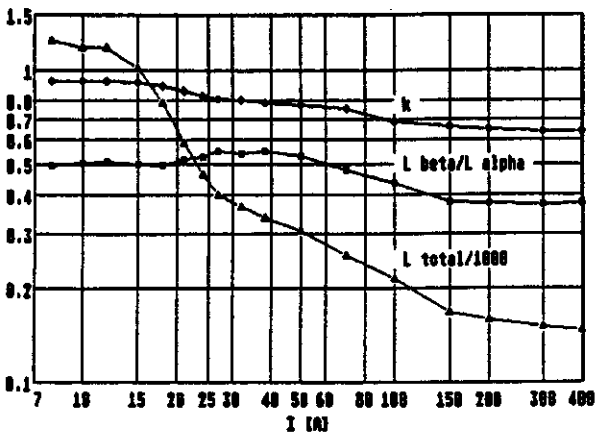


Fig. 4 Inductance ratios from Table III vs. current ($I_\alpha = I_\beta$).

$$I_{eff} = (2 I_\alpha + I_\beta) / 3. \quad (16)$$

This combination of currents is approximately proportional to the central magnetic induction B_0 at high current but has no other significance.

Conclusions

The inductance of the K1200 magnet varies by a factor of approximately 8 over the excitation range 8 A to 400 A when the currents in both coils are equal. At higher currents the inductances remain constant within a few percent as they approach the saturated iron limit ("air

core coils"). The coupling coefficient k varies from .93 at low current to .63 at high current. The maximum rate of change of current depends on both k and the size of the the self inductances and occurs at high excitation. The coil voltages must be driven with opposite polarity voltages. This abnormal condition does not pose a threat to the safety of the coil, considering the response time of the protective circuits.

The stored energy in the magnet was estimated by graphical integration of the data shown in Fig. 3, and these estimates agree with results of a calculation with the program POISSON within 10%.

Temperature Effects

The steel yoke and poles of the magnet are subject to forces from differential thermal expansion. The spiral pole tip is surrounded by water cooled copper trim coil windings. The pole tip temperature is determined by the water temperature and the power in these 21 coils. The pole tip is anchored to the yoke by bolts and dowels. The yoke temperature is approximately equal to the room air temperature, and it varies depending on power to the rf system, etc. Unless the average pole tip temperature is the same as that of the yoke, thermal forces will tend to distort the dowel holes and move the pole tips. An asymmetry of a few mils between pole tips would produce an imperfection in the magnetic field that would damage the beam unless it were cancelled.

The solution to this problem chosen during design of the cyclotron was a temperature regulating system for the trim coil water. Rather than maintaining a constant temperature it uses the magnet yoke temperature as its reference. Thus, as the yoke warms up gradually, typically by 10° F over the first few days of operation, the average pole tip temperature follows this automatically. This

Table III -- Data and results of inductance measurement, 8 to 400 A.

I_α	I_β	I_{eff}	L_α	L_β	M	k	λ	L_{tot}	dia1	dib1	dia2	dib2
[A]	[A]	[A]	[H]	[H]	[H]			[H]	[A/s]	[A/s]	[A/s]	[A/s]
5	14	8	473.6	233.6	310.0	0.932	0.493	1327	0.066	0.062	0.130	0.215
8	8	8	443.1	219.8	289.4	0.927	0.496	1242	0.067	0.061	0.129	0.215 *
6	18	10	453.9	219.7	293.5	0.929	0.484	1260	0.066	0.061	0.131	0.220
8	14	10	423.2	213.3	277.6	0.924	0.504	1192	0.067	0.059	0.132	0.219
10	10	10	419.1	211.8	275.2	0.924	0.505	1181	0.068	0.060	0.132	0.219 *
12	6	10	427.3	213.1	279.2	0.925	0.499	1199	0.068	0.061	0.130	0.217
8	20	12	381.2	189.8	246.4	0.916	0.498	1064	0.069	0.058	0.129	0.220
10	16	12	422.4	206.9	273.4	0.925	0.490	1176	0.068	0.061	0.131	0.221
12	12	12	416.2	211.7	274.2	0.924	0.509	1176	0.069	0.061	0.131	0.217 *
14	8	12	398.2	200.1	260.0	0.921	0.503	1118	0.070	0.061	0.131	0.220
16	4	12	424.5	211.9	277.9	0.927	0.499	1192	0.071	0.065	0.130	0.217
10	25	15	305.0	161.6	199.1	0.897	0.530	865	0.075	0.055	0.129	0.222
15	15	15	363.1	182.6	235.3	0.914	0.503	1016	0.072	0.060	0.130	0.222 *
20	5	15	337.9	171.4	218.4	0.908	0.507	946	0.073	0.058	0.130	0.224
13	28	18	257.8	127.1	159.7	0.882	0.493	704	0.081	0.055	0.125	0.234
18	18	18	286.5	141.9	180.1	0.893	0.495	789	0.078	0.057	0.126	0.229 *
23	8	18	273.3	141.8	174.9	0.888	0.519	765	0.079	0.055	0.129	0.230
16	31	21	199.6	103.1	122.3	0.853	0.516	547	0.091	0.050	0.123	0.242
21	21	21	212.1	110.0	131.4	0.861	0.518	585	0.089	0.052	0.123	0.237 *
26	11	21	225.4	116.3	140.4	0.867	0.516	622	0.085	0.051	0.126	0.238
19	34	24	162.9	84.9	97.4	0.828	0.521	443	0.103	0.048	0.118	0.250
24	24	24	169.8	89.4	102.6	0.833	0.526	464	0.100	0.048	0.120	0.248 *
29	14	24	177.6	94.7	108.7	0.838	0.533	490	0.097	0.048	0.121	0.244
20	41	27	145.8	77.7	86.5	0.813	0.533	396	0.111	0.047	0.115	0.253
27	27	27	145.2	80.1	87.6	0.813	0.551	401	0.112	0.048	0.116	0.250 *
34	13	27	148.1	82.8	90.0	0.813	0.559	411	0.109	0.046	0.117	0.248
24	48	32	132.7	70.7	77.5	0.799	0.533	358	0.117	0.044	0.115	0.263
32	32	32	134.3	72.7	79.4	0.803	0.542	366	0.118	0.047	0.115	0.259 *
40	16	32	135.4	76.4	82.5	0.811	0.564	377	0.123	0.055	0.117	0.254
30	54	38	125.7	65.1	71.7	0.793	0.518	334	0.120	0.041	0.116	0.275
38	38	38	124.7	68.6	73.1	0.791	0.550	339	0.122	0.043	0.116	0.267 *
46	22	38	125.9	69.7	74.2	0.792	0.553	344	0.121	0.043	0.116	0.265
40	70	50	112.6	56.5	61.7	0.773	0.502	293	0.124	0.030	0.118	0.298
50	50	50	115.0	61.1	65.0	0.775	0.531	306	0.124	0.034	0.117	0.285 *
60	30	50	117.6	63.3	67.6	0.783	0.539	316	0.125	0.039	0.119	0.282
60	90	70	100.4	44.5	50.8	0.760	0.444	247	0.123	0.006	0.127	0.350
70	70	70	101.4	48.5	52.9	0.754	0.478	256	0.126	0.014	0.125	0.335 *
80	50	70	104.7	51.6	55.8	0.758	0.493	268	0.125	0.019	0.125	0.325
80	140	100	86.1	34.5	37.8	0.694	0.400	196	0.122	0.040	0.135	0.440
100	100	100	91.6	40.0	41.5	0.686	0.436	214	0.124	0.020	0.133	0.419 *
120	60	100	93.4	42.7	44.4	0.703	0.457	225	0.124	0.011	0.132	0.392
120	210	150	76.6	28.7	31.0	0.661	0.374	167	0.128	0.071	0.135	0.495
150	150	150	76.8	29.1	31.4	0.663	0.379	169	0.129	0.067	0.134	0.488 *
180	90	150	77.9	29.8	32.2	0.667	0.383	172	0.128	0.063	0.134	0.480
120	360	200	73.2	27.0	28.9	0.650	0.369	158	0.132	0.081	0.135	0.515
200	200	200	73.5	27.5	29.4	0.653	0.374	160	0.133	0.076	0.135	0.508 *
280	40	200	74.5	28.5	30.1	0.652	0.383	163	0.133	0.070	0.130	0.489
200	500	300	71.2	27.2	28.0	0.637	0.382	154	0.142	0.073	0.129	0.511
300	300	300	70.2	26.2	27.6	0.643	0.373	151	0.138	0.084	0.134	0.523 *
400	100	300	70.2	26.7	27.8	0.643	0.380	153	0.139	0.080	0.132	0.512
300	600	400	71.5	28.5	28.1	0.622	0.399	156	0.151	0.058	0.123	0.503
400	400	400	68.4	25.8	26.9	0.641	0.377	148	0.141	0.086	0.134	0.525 *
500	200	400	69.8	25.8	27.4	0.645	0.370	150	0.136	0.089	0.136	0.527

system has to be in operation whenever the cooling water is flowing to the trim coils, not just when the power supplies are operating. The control system monitors the difference in temperature between water and yoke and shuts off the water flow automatically if a difference of more than 5^o F is sustained for at least 120 s. The delay accounts for the lag time of the water temperature regulator. Thus the magnet is protected from mechanical damage from thermal expansion if, for example, the cooling system breaks down. Manual intervention is required to restore correct temperatures before trim coil water can be turned on after such an event.

The temperature readings were found to be sensitive to stray rf fields from the nearby transmitters for the dees. This was corrected by installing balanced wiring and shielding for the temperature sensors. The rf fields were also reduced.

Another temperature-related effect on operation of the cyclotron is drift of the magnetic field. We observe a correlation between the frequency of the acceleration voltage required for optimum beam extraction and the temperature of the magnet. The temperature coefficient is -30 to -50 ppm/^oF, and we attribute this primarily to the temperature dependence of the saturation magnetization of the magnet iron.

Modifications to the Magnet

We have added a metal rim (approx. 0.5 inches high) to the top surface of the cryostat just outside the area where the vacuum seal is made. This rim prevents water that may reach the top of the cryostat from flowing up to the vacuum seal and rusting the polished steel surface. One source of water that has made its way to this area in the past is condensation from the helium cooled leads of the magnet, although such condensation is usually

intercepted by a container and drain. Another source is failure of a water hose. Before this water barrier was installed it was not possible to be sure that the vacuum seal surface was dry without venting the vacuum chamber and raising the magnet cap.

Another mechanical improvement is the completion of the controls for moving the pole cap up from the magnet to let workers enter the beam chamber. The controls include interlocks to ensure that all parts of the mechanism are set up for safe movement. For example, the collars that clamp the dees to the stems must be removed before the cap is raised to prevent damage. The logical conditions for raising and lowering the cap are summarized in Table IV.

Table IV -- Cap movement condition table.

	Logic Input Signal	Required for:	
		Raising	Lowering
1	A sliding short at down limit	x	
2	B " "	x	
3	C " "	x	
4	Dee stem stud collars stored		x
5	Jack screws load balanced	x	x
6	A jack load detected		x
7	B " "		x
8	C " "		x
9	Cap not at down limit (0 inches)		x
10	Cap not at up limit (60 inches)	x	
11	A counterweight snag not detected	x	x
12	B " "	x	x
13	C " "	x	x
14	Inflector at retracted limit	x	x
15	A counterweight piston retracted	*	*
16	B " "	*	*
17	C " "	*	*
18	Cap above 55 inches	*	*
19	Cap above 58 inches	*	*
20	Roof jaws at open limit	x	x

* Interlocks marked * interact to determine cap drive enable conditions. Other input conditions must be true as stated in the table to enable the cap drive motor, wherever marked by an 'x'.

LOW VOLTAGE OPERATION OF THE K1200 CYCLOTRON

David A. Johnson and Felix Marti

Introduction

The original design of the K1200 central region was based on the assumption of being able to run the RF system at a voltage close to 200 kV. This first design called for a voltage of 186 kV for the most relativistic ion $Q/A=0.5$ and $E/A=200$ MeV/nucleon at a frequency of 26.5 MHz. The gaps at the center of the machine were kept at 18 mm or larger. Due to difficulties associated with the RF amplifier tubes we felt uneasy about increasing the voltage much higher than 130 kV where it runs without difficulty. This prompted the study of a possible operating mode with lower maximum voltage than our first design.

Extraction Region

The ion phase with respect to the RF voltage changes very rapidly in the last 3 cm in radius before extraction. The main coils and the trim coils are adjusted to keep this phase swing in the range between -30 and $+30$ degrees. Phases outside this range decrease the energy gain significantly, increasing the number of turns needed for acceleration to full energy, making the beam more susceptible to imperfections in the magnetic field and to resonances. Lowering the voltage in the extraction region increases the phase slip of the ions inversely proportional to the RF voltage. We have determined that a 20 per cent decrease in the original design voltage is acceptable from the point of view of keeping the phase within reasonable limits. Figure 1 shows a plot of the sine of the phase versus energy for the most relativistic ion where the voltage was reduced from 186 to 150 kV.

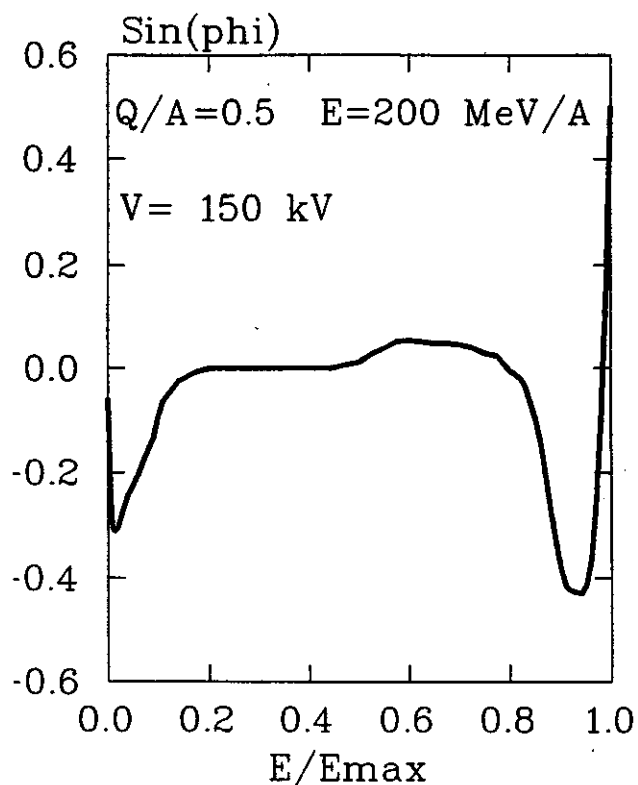


Fig. 1 Phase curve for the most relativistic ion in the new low voltage operating mode for the K1200 Cyclotron.

Central Region

After determining that a voltage of 150 kV is acceptable in the extraction region we tested experimentally the voltage limits we could reach at the center. We installed a copper cylinder approximately where the spiral inflector is placed and varied its distance to one dee (the puller) and increased the dee voltage until sparking occurred. We considered a voltage achievable if sparking conditioned away after two or three minutes. In this mode we could run 150 kV on a horizontal gap of 12 mm (the magnetic field is vertical).

Based on this experiment we decided to design the new central region with gaps of 15 mm and 150 kV for the most relativistic ion (other ions run in constant orbit mode, scaling the voltage). As a first guess we started with the present central region scaling down the dee tips to 0.9 of their size and getting them closer to the center, leaving the inflector unchanged to avoid remanufacturing an expensive and delicate component. After a few modifications, we came to a new central region geometry satisfying our requirements.

CYCLONE runs show that the vertical focusing of the new central region is adequate for starting times in the range of 200 to 235 degrees (where $\tau=270$ is peak voltage) and, for reasonable beam heights, the oscillation frequency is not dependent on amplitude. Centering at turn 100 for a starting time of 220 degrees can be accomplished with a first harmonic of 17 gauss at an azimuth of 240 degrees. The radial-oscillation amplitude grows as the starting time is moved away from 220 degrees at a rate of about 0.004 inches per degree (this is the half-height of the precession ellipse). If the voltage on dee 3 is lowered by ten per cent, the bump required for centering increases to 45 gauss at 273 degrees; it should therefore be possible to do this if necessary to stop sparking at the outer radius of this dee.

Figure 2 shows the median plane orbit path for ions starting at $\tau=210$ and 230.

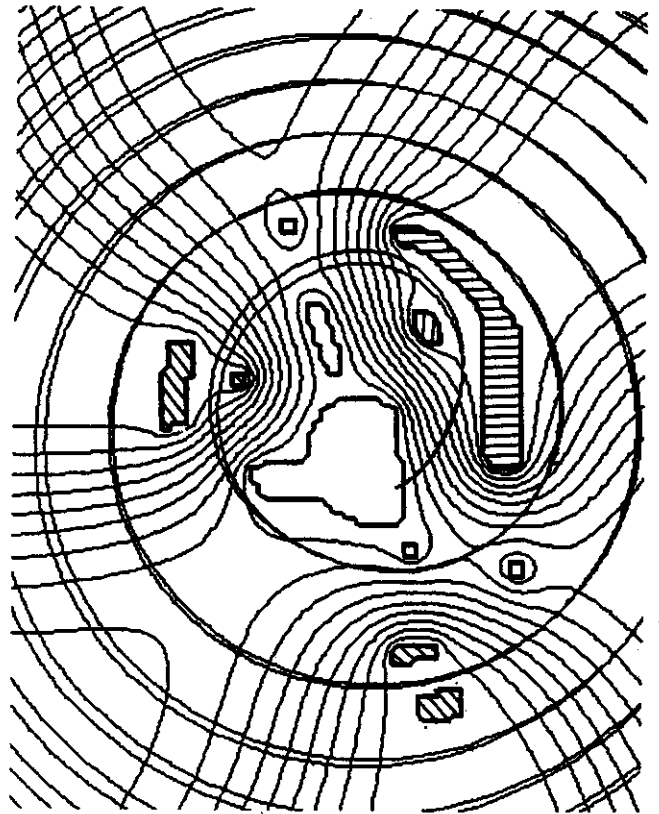


Fig. 2 Median plane orbit for the most relativistic ions in the new low voltage central region in the K1200 Cyclotron. The starting times are $\tau=210$ and 230.

BEAM DIAGNOSTICS

R. A. Blue, J. Kuchar, F. Marti, J.A. Nolen, B. Sherrill and J. Yurkon

The basic diagnostic station in the NSCL final configuration consists of a small chamber (6 inches in diameter) where we can stop the beam, read the total current and examine the beam on a scintillator. We have eleven of these stations (see Figure 1) that complement the larger beam diagnostics chambers described elsewhere.¹ The Faraday Cup consists of a copper block tilted at 45 degrees with respect to the beam path and 2 inches thick. The scintillator mounts in front of the copper block on a thin aluminum plate and a TV camera views the scintillator from above through a window. The TV image can be examined directly with a black and white monitor or through a frame grabber processor where pseudocolor representation and other manipulations (like projections) can be performed.¹ The beam-stop scintillator assembly moves as a unit mounted on a vertical shaft driven by an air cylinder. This system is similar to the one used in the larger chambers and has proven to have a smooth and reliable operation. The vacuum seal on the shaft is obtained with bellows mounted on Conflat flanges. The electrical connections and water cooling lines are routed inside the hollow shaft.

An effort was made to test TV cameras that would be a good match to our frame grabber system. We use a DATATRANSLATION frame grabber system with 512 by 512 resolution running on a microVAX computer. We tested several cameras that were in the market by looking at a resolving power chart, with lenses that had a field of view of approximately 10 cm. The main characteristics we were interested in measuring were linearity, resolution and noise level. In the price range of approximately \$500 to \$1000, the ELMO SE302 CCD camera had the best

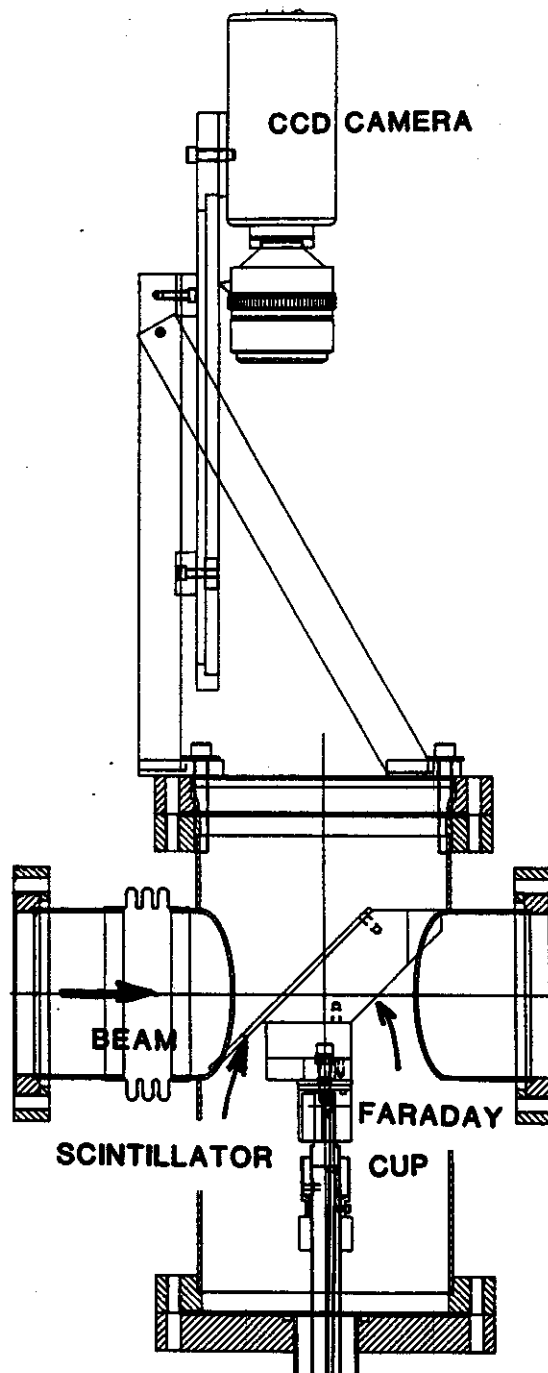


Fig. 1. Small beam diagnostics chamber. The cylindrical tube has a diameter of 6 inches. The copper Faraday cup is tilted 45 degrees with respect to the beam path, and has on its front face a scintillating plate.

performance. We could resolve 2.5 lines per mm. Figure 2 shows a section of a frame where the density profile across the mm ruler (on top of the picture) is plotted at the bottom. The ELMO camera had the best signal to noise ratios, which can be noted by the zero level signal on the black tick marks.

References

1. Beam Diagnostic Developments at NSCL, F. Marti, R. A. Blue, J. Johnson, J. Kuchar, J. A. Nolen, P. Rutt, B. Sherrill and J. Yurkon. Proc. of the 12th International Conference on Cyclotrons and Their Applications, Berlin 1989. To be published.

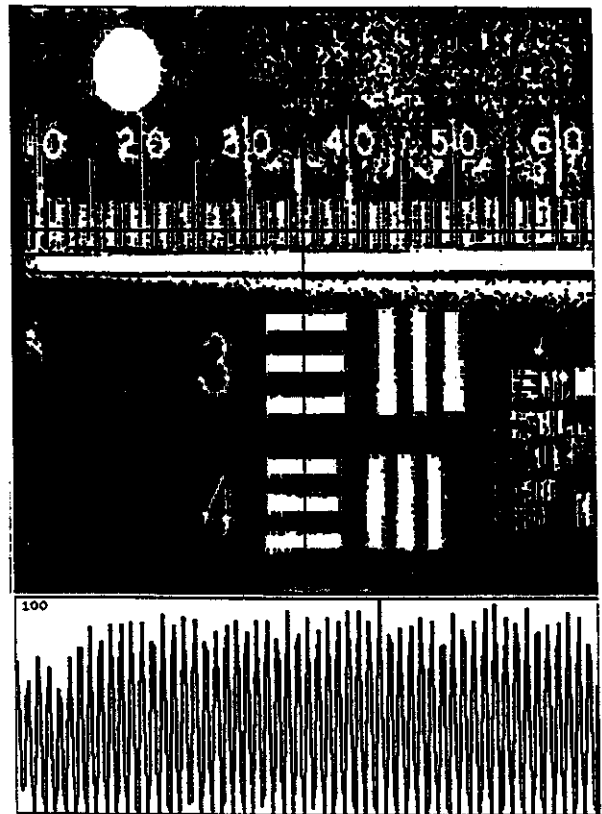


Fig. 2. Section of a TV frame captured with the frame grabber. It is an image of a resolving power chart with a mm ruler on top.

SUPERCONDUCTING BEAMLINER DIPOLES PROGRESS

J.C. DeKamp, C.T. Magsig, J.A. Nolen, A.F. Zeller

The present Phase 2 dipole construction requirements are the same as reported previously¹; two $\pm 16^\circ$ and six 22.5° 'X' dipoles, not including a prototype $\pm 16^\circ$ magnet which already exists and was used successfully during interim vault operations²⁻³; this latter prototype dipole will be the first switching magnet after the A1200 experimental line⁴ in the final Phase 2 beamline system. The prototype magnet is the most inefficient of the beamline magnets built to date (LHe boiloff rate is 0.7 l/hr) the selected location places it next to a beamline cryogenic transfer box in order to make the more frequent refills as efficient as possible.

In addition to the prototype, one $\pm 16^\circ$ dipole, three 22.5° 'X' dipoles of the new construction are presently completed (Feb. 1990). The remaining 4 dipoles have their bobbin cryostat and dewar assemblies completed; all that remains to be done is to assemble the bobbin cryostat to the magnet steel and then couple the dewar assembly to the bobbin cryostat. The newly completed $\pm 16^\circ$ dipole and two of the 22.5° 'X' dipoles are already installed in the transfer hall with cryogenic hookups complete.

The first 22.5° 'X' dipole was tested at the CTI 1400 He liquifier test station. The cooldown time of this magnet took much longer than expected, 9 days, whereas the prototype dipole had taken only 2.5 days to cool down. Once cold, the new dipole operated much more efficiently, however, with its LHe boiloff rate being almost 50% lower than the prototype. The current leads also proved to be more efficient requiring only half the cooling flow of the prototype at a given current and voltage drop. This was due to a design change to increase the

heat transfer efficiency to the cooling gas within the lead by making the flow passage smaller. This increases the gas flow velocity, increasing convective heat transfer rates. The magnet was readily ramped to full field of 17.5 kG at 78 A. Measured and calculated fields for this dipole are shown in Fig. 1. The first coil quench occurred at about 99.5 A. The magnet was then ramped to 19.6 kG at 101 A without quenching. The long cooldown time of the coil bobbin was determined to be due to a smaller feedline connecting the LHe container to the bobbin than in the prototype. The line size was reduced so it would be flexible enough to eliminate the need for a flexible hose or bellows. The LHe feedline first enters the LHe container and a separate line connects the container and the bobbin. This is needed in the batch fill procedure so that if the coil is filled while operating, the initial heat pulse during the LHe feed will not lead to a quench. This means that cooldown of the bobbin in a

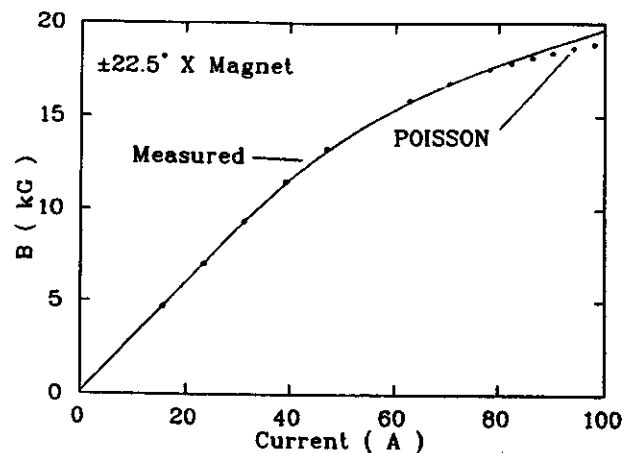


Fig. 1 Measured and calculated central fields for one of the beamline dipoles. The POISSON calculations were done assuming the permeability curve used in calculations for the beamline quads (1003).

reasonable period of time can only be achieved when LHe is used to carry out the cooldown. This provides the pressure head needed to drive the cooldown. This problem can be circumvented with the addition of another valve, but this could raise the heat load to the LHe container by as much as a factor of 3. The remaining dipoles have this line changed back to the same size as the prototype. Testing of the next completed dipole, the $\pm 16^\circ$, showed cooldown time to be about 2.5 days as expected. It's cryogenic efficiency and magnet operation were consistent with the first 22.5° 'X' magnet.

The long cooldown time of the first dipole tested should not be a problem in practice as the magnet will seldom ever be warmed above LN2 temperature. Successful operation of the prototype in the interim vault confirms this assumption. This magnet can be cooled from 77°K in 3 days.

References

1. J.C. DeKamp et al., MSU Annual Report, 1988, 157.
2. J.C. DeKamp et al., MSU Annual Report, 1988, 154.
3. B. Sherrill et al., MSU Annual Report, 1987, 183.
4. B. Sherrill et al., MSU Annual Report, 1987, 190.

PHASE II DISCRETE CONTROL SYSTEM - USER INTERFACE

G. Humenik

The challenge of creating the switching software for use in controlling the Phase II beamline magnets, vacuum system, and beam diagnostic hardware is intimately dependent upon the types of user interfaces available. The use of programmable logic controllers (PLC) at NSCL has provided a simple yet versatile method to establish conditions for device operation. However, it is the ability of the cyclotron users to both monitor and control these device states that has undergone the most extensive change. A short summary of the most important current methods of monitor and control of discrete state devices follows.

1. User Control through hardware I/O (Pushbuttons and Lamps)

This is the old standby, the only method available to those limited to logic control with physical relay hardware. When the PLC first came into use at NSCL, this method was still the only one used, albeit 24V DC was substituted for 120V AC and the lamps became LEDs.

This can be an expensive interface. Both the up-front cost of PLC I/O hardware as well as the shop cost for fabrication of button/LED panels can mitigate its one distinct advantage: speed. It is the fastest method for informing the PLC of one's wishes, but this must be weighed against the significant hassles of documenting and possibly changing field hardware requirements in the event of facility upgrade projects (as in Phase II).

The best examples of this hardware are the K500 vacuum station, and the N3 (92") local control console.

2. User Control through 9600 baud serial ports

a. Dumb ASCII terminals connected to PLC ASCII ports

The first attempt to bypass the hardware I/O approach utilized the ability of the in-house PLC (Modicon 584) to read and write to a VT-100 terminal. This was done in the initial S320 and K50 vault vacuum valve control logic, allowing the operator to type "OPEN VALVE" commands at a terminal to execute the command. While functional, ASCII programming in the PLC is primitive at best, and the availability of only 4Kbyte of PLC memory for this purpose was another strong constraint. Currently, this method is only used for PLC output, in the rather amusing form of a device which takes the ASCII output of alarm messages and attempts to speak them in English to the cyclotron operator (as an alarm, it is compelling; but as communication it is confusing, so these messages are also sent via a Decserver port to a control room printer).

b. Smart programmable terminals connected to PLC ModBus ports

1. PanelMate

The availability of a 9600 baud port into the PLC which could be directly read/written by a master device (ModBus port) was not utilized for control purposes until the lab acquired an IDT PanelMate in 1985. This color graphics display device with 5 user-defined pushbuttons mapped to any of 15 display templates has revolutionized PLC programming at NSCL. The ease and speed with which device control may be established and modified has allowed frequent

changes to accommodate various users' beamline hardware requirements. Also, the PanelMate approach has added another layer of operator warning capability, one that is nearly effortless to alter upon demand. Only fifteen different PLC states are visible on any one page, however. Also, the user has no implicit knowledge of what page to use or even if a desired device is controlled by a given PanelMate. Current placement of these devices is: K1200 RF console, K1200 Vacuum racks, ECR console, South Hall, N2 (4Pi) Vault, and one Data U.

2. PaneLogic

The next ModBus-compatible device was acquired with the idea of local vault control of valves, etc. at lower cost than the \$5K PanelMate. At a price of \$1.8K, NSCL acquired the ability to have 24 pushbuttons and 24 tri-state LEDs (On/Off/Blink) per/drop on an RS-485 loop using only one PLC ModBus port, expandable to 16 such drops. While not as flashy as a color graphics device, most of the programming of the device occurs in the PLC which treats PaneLogic I/O as if it were hardwired. We currently have two hardware drops to use: since the manufacturer is out of business no more are contemplated. The speed of response is limited by the average response time of the ModBus port multiplexor (2 - 5 secs). PaneLogic is used in the N1 (S320) vault for local control, and will be used in the N4 vault.

3. Metra

With the advent of Phase II, where at least ten different beam paths are foreseen, the PanelMate programming for a given run will have to be changed often to accommodate the many different permutations to be used. Also the sheer volume of information now desirable makes the low display density of the PanelMate a hinderance to achieving the "overall picture" of

the cyclotron by the operators. Another \$5K ModBus device, the Metra 1010BT, is being implemented to achieve an integrated user-interface allowing one operator to effectively communicate with the four different PLCs controlling the two cyclotrons and the beamlines into the five beam vaults.

The key to this approach is to create a database inside the Metra that includes PLC references as well as conditions derived from those references. The power of this database approach is its generality: all four PLC references of interest can now be collected in one box. This database can be displayed on the Metra's color graphics screen (programmable with CAD-style software on a PC). The database can transfer values from itself into any PLC, and can let the PLC determine which page is displayed. Furthermore, the database may be itself read/written by a "smart" device (i.e. VAX) using a simple protocol, so the Metra can be considered a 256K buffer box. Provisions for alarm and alert generation and documentation are also built in, and may supplant the current system.

Initial Metra displays have looked a lot like pushbutton and LED boxes. This is due to the interface philosophy that "denser is better": as fewer pages are used to describe more information, user response time is shortened. Complex graphics such as beamline schematics can be generated, but at a tradeoff of information density. There currently exists a single database of ~7000 elements (mostly PLC references) upon which a library of 12 pages has been created on a PC and uploaded to the three Metra units in-house.

One Metra is currently installed at the K500 console, with another to be installed at the K1200 console, and the third in the Analysis Hall control racks.